ELSEVIER

Journal of Structural Geology 26 (2004) 1109–1125

JOURNAL OF STRUCTURAL GEOLOGY

www.elsevier.com/locate/jsg

The St Ives mesothermal gold system, Western Australia—a case of golden aftershocks?

S.F. Cox[a,*], K. Ruming[b]

[a]*Research School of Earth Sciences and Department of Geology, The Australian National University, Canberra, ACT 0200, Australia*
[b]*Discipline of Geology, The University of Newcastle, Callaghan, NSW 2308, Australia*

Received 12 November 2002; received in revised form 25 June 2003; accepted 25 July 2003

Abstract

The late orogenic evolution of the Archaean greenstone sequence in the Eastern Goldfields Province of the Yilgarn Craton in Western Australia is characterised by strike-slip tectonics and locally very high, fault-controlled, fluid fluxes. Fluid flow was associated with the formation of many fault-hosted and shear-zone-hosted gold deposits, which are commonly clustered adjacent to high displacement faults or shear zones. In the St Ives goldfield, near Kambalda, fluid flow in a gold-producing hydrothermal system was localised within arrays of low displacement faults and shear zones, which form part of the NNW trending, crustal-scale, Boulder–Lefroy fault system (BLFS). The numerous ore-hosting structures are kinematically related to sinistral to sinistral–oblique slip on the Playa Fault, which is a 20-km-long splay of the 200-km-long Boulder–Lefroy Fault. Most of the known gold mineralisation at St Ives occurs within an area of 20 km^2 immediately south-west of the Playa Fault. The distribution of low displacement faults and shear zones that host gold mineralisation is related to the presence of a kilometre-scale contractional jog (the Victory jog) and an associated imbricate thrust array on the Playa Fault. By analogy with modern seismogenic systems, the low displacement structures that localised fluid flow and gold mineralisation in the St Ives goldfield are interpreted as aftershock structures whose development was driven by major slip events on the BLFS. For large slip events on the BLFS, and mainshock rupture arrest at the Victory jog, modelling of co-seismic static stress changes indicates that most ore-hosting structures are localised within a crustal volume whose stress state was closer to failure as a consequence of Coulomb stress transfer. The modelling supports an interpretation that aftershock networks can form a high permeability damage zone that localises fluid flow and gold mineralisation within particular parts of crustal-scale fault systems. Both co-seismic stress transfer and time-dependent changes in fluid pressures, during post-seismic fluid redistribution, are implicated in driving the growth of low displacement, gold-hosting fault networks in the St Ives goldfield. Stress transfer modelling has application for area selection in exploration programs targeting mesothermal gold systems. Clustering of deposits hosted by aftershock fracture networks is favoured by the presence of major, long-lived jogs or bends that can repeatedly arrest ruptures propagating along high displacement faults.

Keywords: Mesothermal gold deposits; Faults and shear zones; Structural controls; Fluid flow; Stress transfer modelling

1. Introduction

Mesothermal lode gold deposits are particularly well-developed in Archaean greenstone sequences such as in the Yilgarn Craton in Western Australia (Groves et al., 1995), the Superior Province of Canada (Roberts, 1987) and in Zimbabwe (Foster, 1989). These deposits are typically localised in low displacement faults and shear zones (Groves et al., 1995; Cox, 1999; Robert and Poulsen, 2001) that have maximum displacements up to several tens of metres. The lode-hosting structures form part of larger, crustal-scale fault systems, and are usually located within a few kilometres of high displacement faults (e.g. Clout et al., 1990; Robert et al., 1995; Robert and Poulsen, 2001). For example, in the Eastern Goldfields Province of Western Australia, the source of most of the gold production in the Yilgarn Craton, many deposits are clustered adjacent to large strike-slip structures such as the Boulder–Lefroy Fault and the Keith–Kilkenny Fault (Fig. 1). Most Phanerozoic mesothermal gold deposits have overall similarities to Archaean ones and also occur in low displacement faults or shear zones that were active during ore formation (e.g. Knopf, 1929; McKeag and Craw, 1989; Cox et al., 1991; Goldfarb et al., 2001).

The formation of lode gold systems requires that large

* Corresponding author. Tel.: +61-2-6125-0045; fax: +61-2-6125-3418.
E-mail address: steve.cox@anu.edu.au (S.F. Cox).

0191-8141/$ - see front matter © 2004 Elsevier Ltd. All rights reserved.
doi:10.1016/j.jsg.2003.11.025

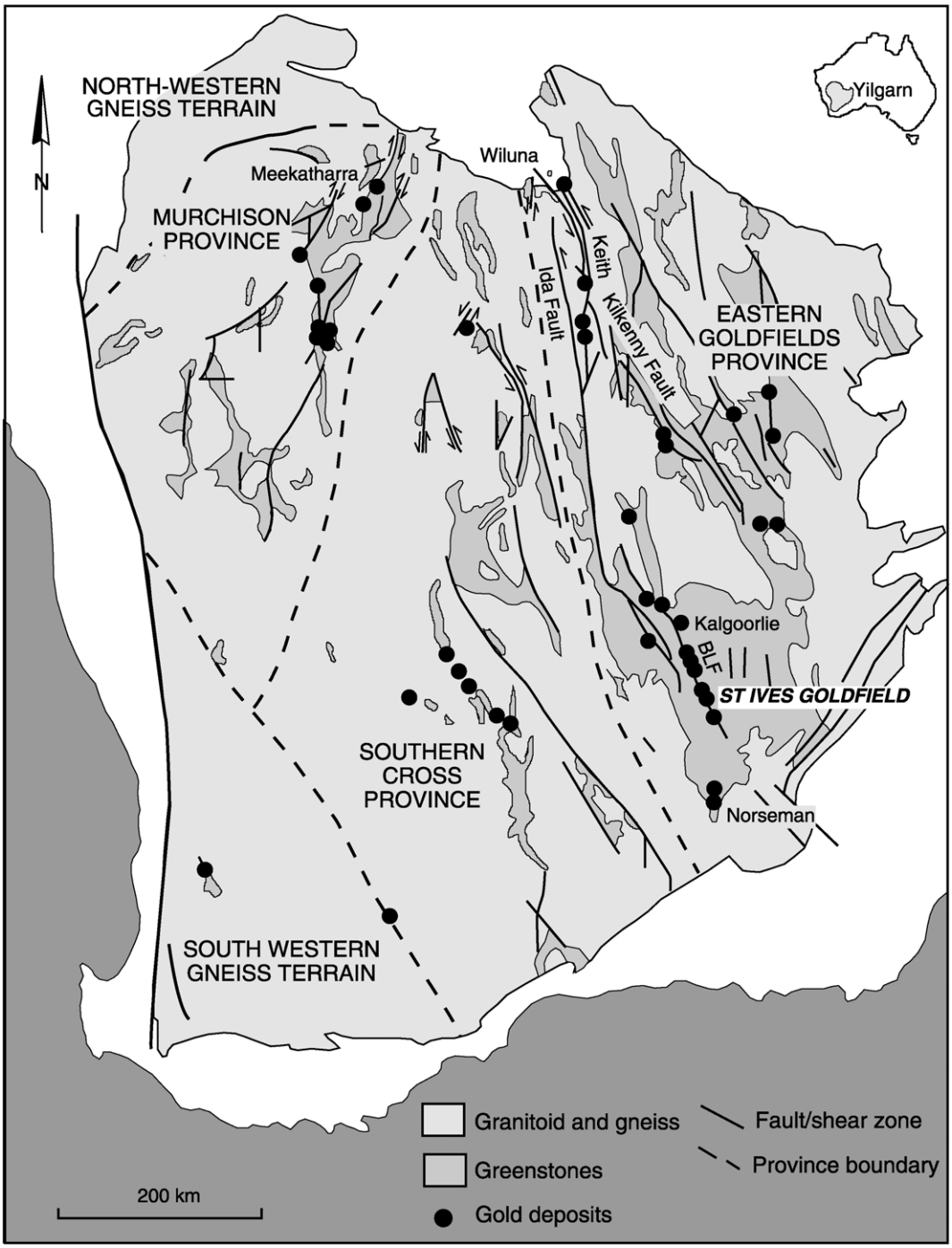

Fig. 1. Distribution of major gold deposits in the Archaean Yilgarn Craton of Western Australia (modified after Groves et al. (1989)). BLF, the Boulder–Lefroy fault system. The location of the St Ives goldfield is indicated.

fluid fluxes were localised in the hosting faults and shear zones while they were actively deforming and thus permeable (Cox et al., 2001). They typically form at depths within the continental seismogenic regime, or just below the seismic–aseismic transition, and at temperatures usually in the range 300–450 °C (Sibson et al., 1988; Groves et al., 1995; Cox, 1999).

Large-scale factors controlling distribution of fluid flow and related gold deposits within crustal-scale shear systems are poorly understood. There are two intriguing questions concerning the localisation of mesothermal gold systems. Firstly, why are they developed predominantly within low displacement faults and shear zones adjacent to much larger shear zones, rather than in the major, crustal-scale shears themselves? Secondly, why do the deposits commonly occur in clusters, typically along small segments of much larger crustal-scale shear systems? Recent advances in understanding how modern seismogenic systems operate at

mid- to upper-crustal depths in the continental crust have the potential to answer these questions and provide further insights about the development of mesothermal gold systems, as well as controls on the distribution of fluid flow within crustal-scale fault systems in general.

By analogy with modern seismogenic systems, Robert et al. (1995) and Cox et al. (2001) proposed that low displacement faults and shear zones, which commonly host mesothermal gold deposits, are repeatedly reactivated aftershock structures which formed around larger faults or shear zones. Simple elastic–frictional modelling of stress changes associated with major earthquake ruptures in modern seismogenic systems has in many cases successfully modelled the distribution of aftershock activity and demonstrated that aftershocks tend to cluster in particular areas around the mainshock rupture surface (e.g. Stein, 1999). This modelling approach is known as 'stress transfer modelling'.

If lode gold systems are hosted by aftershock structures, then stress transfer modelling techniques have potential application for understanding the distribution and clustering of gold deposits within crustal-scale fault systems. The techniques may also have application in developing exploration strategies for a variety of epigenetic, fault-related mineralisation styles.

This paper examines the relationships between low displacement, gold-hosting faults and shear zones, and co-active, kinematically-related, high-displacement shear zones in the St Ives goldfield of the Eastern Goldfields Province of the Yilgarn Craton in Western Australia. In particular, we investigate the distribution of gold-hosting faults and shear zones within the larger, crustal-scale shear system, and show how the formation of low displacement gold-hosting structures was driven by strain accommodation around a major contractional jog in a high displacement shear zone. 3D Coulomb stress transfer modelling is used to test whether the distribution of gold deposits in the St Ives goldfield is consistent with their formation in an aftershock network whose location is controlled by stress transfer associated with repeated arrest of large ruptures at the contractional jog.

This case study provides a basis for understanding the relationships between gold deposits, the development of low displacement and high displacement structures, and fluid redistribution in active, crustal-scale shear systems. The study also illustrates the potential of stress transfer modelling for targeting where gold systems may develop within major fault systems.

2. Stress transfer modelling—the background

2.1. Behaviour of modern seismogenic systems

In modern, crustal-scale fault systems, such as the San Andreas Fault system in California, and the Anatolian Fault system in Turkey, major earthquakes are localised on the large, high displacement parts of the systems. In the continental crust, major earthquakes with moment magnitudes of 6–7 typically rupture 20–100-km-long fault segments down to depths of 15–20 km (Wells and Coppersmith, 1994; Yeats et al., 1997). Individual major faults can be active over time scales longer than 10^5 years, with total displacement accumulating during several thousand separate rupture events. Successive rupture events can be distributed either with apparent irregularity along faults, or they can migrate along faults with time, as is the case in the North Anatolian Fault (Stein et al., 1997). However, in many cases, similar magnitude earthquakes (so-called 'characteristic' earthquakes) have been observed to occur repeatedly along the same fault segment (Aki, 1984; Schwartz and Coppersmith, 1984). One factor that may influence the recurrence of characteristic earthquakes is structural segmentation of faults. Segmentation is associated with changes in strike (fault bends), or presence of linking structures such as jogs (both contractional and dilational) that, for a time, can act as geometric barriers to rupture propagation. They can repeatedly localise rupture arrest at segment boundaries (Segall and Pollard, 1980; Aki, 1984; King, 1986; Sibson, 1986, 1990; Harris et al., 1991).

Crustal-scale faults in modern seismogenic regimes are typically associated with arrays of smaller, low displacement faults. Slip on the low displacement faults usually occurs during aftershock activity following large ruptures on the high displacement faults. This activity typically commences immediately following the mainshock, and can continue for many decades to hundreds of years after the mainshock. Aftershocks are interpreted to be triggered by stress changes which occur in response to slip and elastic strain release along the high displacement 'driving' structure (King et al., 1994). Aftershocks are usually not distributed uniformly around the mainshock rupture area, but commonly concentrate in particular areas around, rather than within, the mainshock rupture surface (Yeats et al., 1997). Significantly, faults on which aftershocks nucleate do not necessarily have the same geometry and sense of slip as the associated mainshock rupture. For example, the dextral Loma Prieta earthquake on the San Andreas Fault in 1989 was associated with thrust, normal, sinistral and dextral aftershocks (Beroza and Zoback, 1993). This may be partly because elastic strain release and stress redistribution during mainshocks can transiently change the magnitudes and orientations of post-rupture principal stresses around fault ruptures. Additionally, the perturbed, post-seismic stress field can reactivate small faults whose geometry is not optimally-oriented with respect to the stress field.

2.2. Coulomb stress transfer modelling

Simple elastic–frictional mechanical modelling has been used successfully to explore co-seismic stress changes and how these influence the distribution of aftershocks around

mainshock ruptures (King et al., 1994; Harris, 1998; Stein, 1999). This type of modelling is termed Coulomb stress transfer modelling.

Mainshock ruptures transiently reduce the average value of shear stress along slipped fault segments. However, this also causes changes to stress states in a domain around the co-seismic slipped fault segment. These stress changes can bring the stress states on potentially aftershock-hosting faults either closer to or further from failure. Using Coulomb failure assumptions that closely approximate the mechanical behaviour of faults in the seismogenic regime (Jaeger and Cook, 1979), the shear strength, τ_s, of a fault is described by the relationship:

$$\tau_s = C + \mu(\sigma_n - P_f) \quad (1)$$

where C is the cohesive strength, μ is the coefficient of friction, σ_n is the normal stress and P_f is the fluid pressure. σ_n is a function of the principal stresses, σ_1 and σ_3 and the angle between the fault and the principal stresses. Compressive stresses are taken to be positive.

Fault slip on aftershock structures occurs where, as a consequence of mainshock imposed stress changes (and potentially also, fluid pressure changes), the shear strength, τ_s, becomes equal to the imposed shear stress, τ. A simple measure of proximity of a stress state to that required for failure on a fault is provided by a parameter, known as the Coulomb failure stress (CFS), which is the difference between τ and τ_s for faults of a specified orientation (Fig. 2). Changes in CFS indicate whether the stress state on a potentially aftershock-hosting fault has moved closer to or further away from failure. The change in CFS (ΔCFS) is thus:

$$\Delta\mathrm{CFS} = \Delta\tau - \mu(\Delta\sigma_n - \Delta P_f) \quad (2)$$

where $\Delta\tau$ is the shear stress change on the fault, $\Delta\sigma_n$ is the change in normal stress and ΔP_f is the pore pressure change in the fault. It is assumed μ and C remain constant.

The modelling approach used here assumes an 'undrained' pore fluid condition in which sudden, co-seismic changes in stress states drive changes in fluid pressure via poroelastic effects (Rice and Cleary, 1976). Accordingly, stress changes are assumed to occur so rapidly that significant pore fluid migration does not occur. For plausible fault zone rheologies it is assumed that changes in fluid pressure are proportional to changes in fault-normal stress, such that:

$$\Delta P_f = B\Delta\sigma_n, \quad (3)$$

where B is a parameter known as Skempton's coefficient (Cocco and Rice, 2002). This coefficient is an empirically determined constant that is a measure of the fraction of the imposed stress on a porous rock that is transferred to the pore fluid (Wang, 1993). B typically has a value between 0.5 and 0.9 (King et al., 1994; Cocco and Rice, 2002).

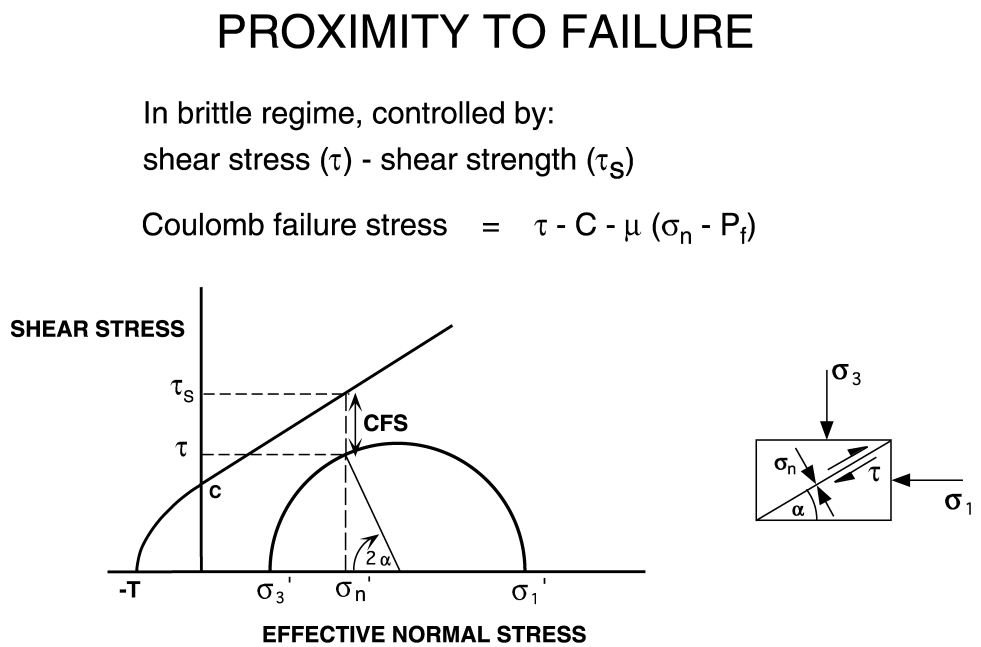

Fig. 2. Mohr diagram illustrating a brittle failure envelope for intact rock failure, and an arbitrary stress state in a rock mass. The shear failure criterion is given by the relationship $\tau_s = C + \mu(\sigma_n - P_f)$. T is the rock tensile strength, C is the cohesive strength. Principal stresses are indicated by the Mohr circle with diameters at effective principal stresses σ_1' and σ_3'. The value of shear stress (τ) acting on an optimally-oriented failure plane inclined at angle α to σ_1 is indicated. Failure occurs when the Mohr circle touches the failure envelope. Proximity of stress state to failure is given by the Coulomb failure stress (difference between the shear strength τ_s and the shear stress τ) for given σ_1' and σ_3'. Changes in σ_1' and σ_3' as a consequence of mainshock rupture move the Mohr circle to the left or right, and also change its diameter, leading to changes in the Coulomb failure stress.

Eq. (2) can accordingly be rewritten as:

$$\Delta\mathrm{CFS} = \Delta\tau - \mu'\Delta\sigma_\mathrm{n} \quad (4)$$

where

$$\mu' = \mu(1 - B) \quad (5)$$

and μ', the 'apparent friction coefficient', is generally less than 0.75. A typical value is approximately 0.4 (Stein et al., 1997; Cocco and Rice, 2002).

If the mainshock fault slip direction and magnitude of the mainshock slip are known, together with the position and geometry of the mainshock rupture surface, ΔCFS can be calculated for potentially aftershock-hosting structures of various orientations as a function of position relative to the mainshock structure. Calculations of changes in CFS can be performed using 3-D boundary element modelling techniques (King et al., 1994; Stein, 1999). A crust with homogeneous elastic and frictional properties is assumed.

In this study, changes in CFS are modelled in 3-D using the finite element software Coulomb 1.0 (Okada, 1992; King et al., 1994; Toda et al., 1998). Fig. 3 provides an example of a plan view of modelled changes in CFS due to slip of 1 m on an approximately optimally-oriented, 40-km-long, dextral fault. In this example, the ΔCFS has been calculated for strike-slip aftershock faults that are optimally-oriented (terminology of Sibson (1985)) with respect to the post-mainshock orientation of the maximum principal stress. The patterns of static stress change in such models

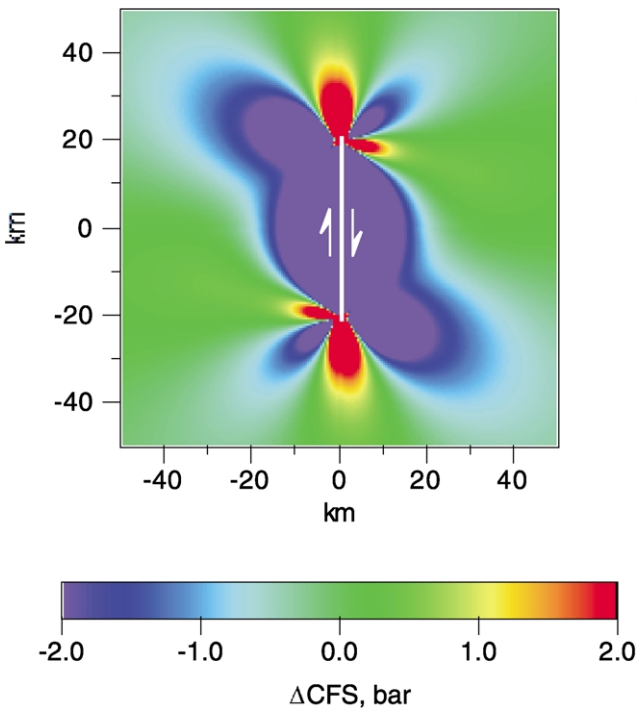

Fig. 3. Plan view of changes in Coulomb failure stress for 1 m of slip on a near-optimally-oriented, 40-km-long, dextral strike-slip fault. Fault dip is vertical. Model is calculated for $\mu' = 0.4$ and stress difference ($\sigma_1 - \sigma_3$) of 40 MPa at depth of the plan view. Positive ΔCFS corresponds to increased proximity to failure.

are not very sensitive to modest changes in the value of apparent friction, but are significantly influenced by changes in magnitude of mainshock slip, the direction of slip, orientation of the stress field, stress difference ($\sigma_1 - \sigma_3$), and the orientations of faults which host aftershocks. For the scenario modelled in Fig. 3, aftershock reactivation of low displacement strike-slip faults is expected to be highest within the major lobes of positive ΔCFS developed around the ends of the mainshock rupture surface. Substantially less aftershock activity is expected in the domains of negative ΔCFS. The distribution of the lobes of positive ΔCFS resulting from sinistral strike-slip mainshocks is symmetrically opposite to that for dextral mainshocks. As major lobes of positive ΔCFS are located near each end of the mainshock rupture surface, successful modelling of stress transfer and related aftershock distribution in fault systems is critically dependent on identifying where ruptures have arrested in a high displacement fault system.

The spatial patterns of static stress changes calculated for mainshocks using Coulomb failure criteria correlate highly with spatial patterns for aftershocks (e.g. King et al., 1994; Harris, 1998; Stein, 1999). Typically, more aftershocks occur where the Coulomb stress changes have moved stress states on faults closer to failure (positive ΔCFS). Less aftershock activity occurs where mainshock-related stress changes on faults have moved stress states away from failure (negative ΔCFS). Even though the crust is typically mechanically heterogeneous, the strong correlation between aftershock distribution and modelled stress transfer indicates that the model assumption of brittle–frictional behaviour in a mechanically homogeneous crust is a very good approximation.

Interestingly, the calculated static stress changes induced by co-seismic slip are generally small, being of the order of a few bars (Fig. 3). The correlation between modelled static stress changes and aftershock distributions may therefore indicate that the continental crust in seismically active areas tends to be very close to failure.

In applying stress transfer modelling to examine potential aftershock clustering and the role of aftershock networks for influencing post-mainshock fluid redistribution within ancient fault systems, the following factors need to be considered:

a. Which faults or shear zones have localised the large slip events?
b. What are the slip directions on these structures?
c. What are the probable slip magnitudes and rupture lengths during individual slip events along high displacement structures? Scaling relationships between rupture length and maximum slip (e.g. Wells and Coppersmith, 1994) are particularly useful here.
d. Where is rupture arrest most likely to have occurred?

The last factor is particularly critical. Mesothermal gold deposits develop over an extended time, involving hundreds to thousands of fault/shear zone reactivation events (Boullier and Robert, 1992; Robert et al., 1995; Cox, 1995, 1999). Accordingly, the best potential for the development of a long-lived fracture-controlled hydrothermal system will occur where an aftershock network is repeatedly reactivated in the one area and taps into a hydrothermal reservoir. This will occur most effectively if mainshocks on a high displacement fault or shear zone repeatedly arrest at long-lived barriers to rupture propagation such as jogs or major bends.

In the following sections we describe the geological setting of gold deposits in the St Ives goldfield, and use stress transfer modelling to investigate spatial relationships between distribution of gold deposits and Coulomb stress changes which may have been associated with slip on a high displacement fault zone in the area.

3. Geological setting of the St Ives goldfield

3.1. Stratigraphy and structural evolution

The St Ives goldfield is located approximately 70 km SSE of Kalgoorlie, and immediately south of Kambalda in Western Australia (Fig. 1). It is the second largest gold-producing district in the Eastern Goldfields Province of the Yilgarn Craton and has a combined production and resource in excess of 300 tonnes of gold (Watchorn, 1998).

The St Ives goldfield is bounded on its eastern side by the regionally-extensive Boulder–Lefroy Fault (BLF) (Fig. 4). Gold mineralisation is localised along networks of mixed brittle–ductile shear zones. Most of the economic gold deposits contain 10–50 tonnes of gold each. Much of this gold occurs in hydrothermally altered wall-rock adjacent to faults, shear zones and associated quartz–carbonate vein arrays, rather than in the veins themselves.

The host-rocks to the St Ives gold deposits comprise a several-kilometre-thick sequence of metamorphosed Archaean komatiite and basalt flows, together with minor interflow sediments (Roberts and Elias, 1990). These are overlain by felsic to intermediate volcanics and volcaniclastics. The sequence is intruded by numerous dolerite sheets that are up to several hundred metres thick. The Archaean greenstone sequence, the dolerites and the overlying felsic to intermediate volcano-sedimentary assemblage formed between approximately 2.71 and 2.68 Ga (Watchorn, 1998). The sequence was intruded by several suites of felsic to intermediate intrusives at approximately 2.65 Ga.

The Archaean volcano-sedimentary succession at St Ives has undergone a polyphase deformation history. Despite this, strains away from major shear zones are typically low. D_1 deformation involved large-scale, north-directed thrusting and stratigraphic repetition with some associated,

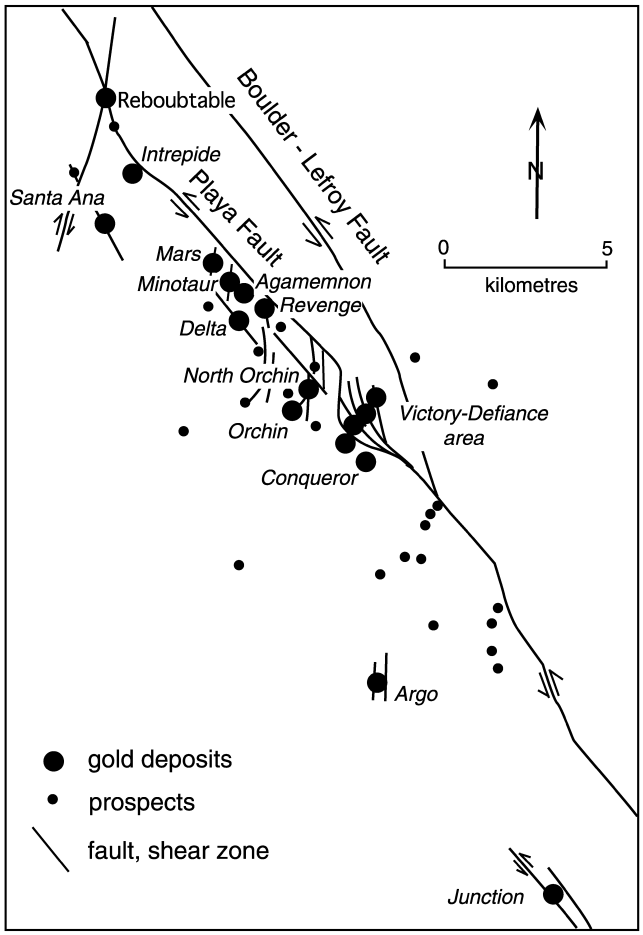

Fig. 4. Simplified map illustrating the geometry and distribution of D_3-active faults and shear zones, including the Boulder–Lefroy Fault, the Playa Fault and various lode-hosting faults in the Kambalda region. Locations of major gold deposits in the St Ives goldfield are shown, with names in italics. Modified after Watchorn (1998) and Nguyen et al. (1998).

kilometre-scale, open to close recumbent folding with short overturned limbs (Nguyen et al., 1998). The D_1 structures are overprinted by upright and open, NW-trending D_2 folds and associated reverse faults and shear zones.

Cross-cutting relationships indicate that the 2.65 Ga felsic to intermediate intrusives probably have been emplaced late during D_2 (Watchorn, 1998). Peak metamorphic conditions at mid- to upper-greenschist facies appear to be broadly contemporaneous with D_2.

D_3 deformation is marked by the onset of a transpressional regime in which deformation was localised mainly along NW- to NNW-trending sinistral shear zones. In the St Ives area, the dominant structures active during D_3 are the Boulder–Lefroy Fault and a splay structure, the Playa Fault (Nguyen et al., 1998) (Fig. 4). At the surface, these structures are generally steeply-dipping and are associated with strong foliation development. Shear zone foliations are defined by retrograde, low- to mid-greenschist facies metamorphic assemblages. Data from drill-core and limited exposure of the Playa and Boulder–Lefroy Faults in the

St Ives area indicates that stretching lineations are predominantly gently to moderately plunging. Nguyen et al. (1998) demonstrated oblique sinistral-reverse slip on a steeply east-dipping part of the Playa Fault. Strike separations and dip separations of stratigraphy across the fault are also consistent with a predominantly sinistral shear sense. The Playa Fault splays from the BLF just SE of the Victory–Defiance group of gold deposits and extends NW for about 20 km where it apparently dies out. Cross-cutting relationships between the Playa Fault and post-D_2 felsic dykes in the Victory–Defiance area indicate that at least part of the Playa Fault was active during D_2 deformation. However, a large part of the slip history occurred during D_3 after emplacement of felsic intrusives.

3.2. Structural controls on gold mineralisation

Gold mineralisation at St Ives formed during D_3. Many of the gold deposits are hosted by faults and shear zones that are spatially and kinematically related to D_3 displacement on the Playa Fault (Fig. 4). These deposits occur in low displacement brittle–ductile shear zones which are interpreted as splays and linked fault/shear networks in a 2-km-wide zone west of the Playa Fault. The total displacement on the north-west-trending Playa Fault is poorly constrained, but may be up to several kilometres. In contrast, ore-hosting structures in individual deposits such as Revenge, North Orchin, Argo and much of the Victory area, are predominantly N–S striking, moderately to gently east-dipping or west-dipping reverse faults and shear zones with maximum displacements of a few tens of metres (Figs. 5 and 6). Strike lengths of ore-hosting structures are seldom more than about 1 km. The orientations of stretching lineations, curvature of shear zone foliations, associated gently-dipping extension veins, and stratigraphic separations, all indicate a reverse slip sense for most D_3 ore-hosting structures, especially in the Argo–Victory–Revenge area (Nguyen et al., 1998; authors' unpublished data). The geometries of faults and associated extension veins indicate formation in a stress regime in which the far-field maximum principal stress was approximately east–west and horizontal. The ore-hosting faults and shear zones at St Ives have orientations that are typically nearly optimally-oriented for slip during D_3.

In the Victory–Defiance area, ore is localised along an apparently imbricate series of moderately to gently dipping, low displacement thrusts (Victory thrust complex) (Fig. 7). The Playa Fault here (known locally as the Repulse Fault in the Victory–Defiance mine area) has a ramp–flat–ramp geometry. A number of low displacement, ore-hosting thrusts splay from the Playa Fault into its hanging wall where it is more gently dipping. To the west, where the Playa fault forms a more steeply-dipping ramp, low displacement, ore-hosting thrusts occur in the footwall of the Playa (Repulse) Fault and host the Defiance and Conqueror lodes (Fig. 7). On the eastern side of the Victory thrust complex, two major ore-hosting structures (the Orion–Britannia and Sirius shear zones) exhibit mixed thrust and sinistral shear sense (authors' unpublished data). These two structures probably splay from a deeper level of the Playa Fault.

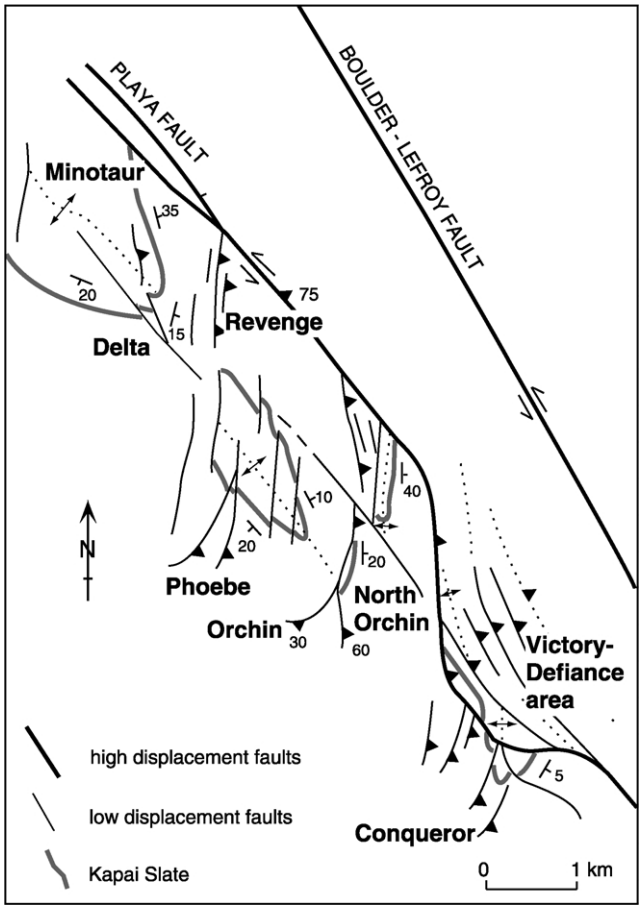

Fig. 5. Fault geometry and distribution in the central part of the St Ives goldfield. The deposits of the Victory–Defiance area are located in an imbricate thrust complex developed within a contractional jog on the largely sinistral Playa Fault. Other deposits (indicated) are localised predominantly on approximately N–S-trending reverse faults in a contractional domain north-west of the Victory jog.

The geometry and kinematics of the Victory thrust complex, and its geometric relationship with the Playa Fault indicate that the thrust complex developed within a jog on the Playa Fault, to the NW of where it splays from the BLF. The overall NW trend and predominantly sinistral shear sense on the Playa Fault, as well as the thrust to oblique thrust-sinistral shear sense on low displacement faults within the imbricate thrust complex, are interpreted to indicate that the gold mineralisation here is localised within a kilometre-scale contractional jog (the Victory jog) which was active during D_3 and the contemporaneous hydrothermal alteration and gold mineralisation. This relationship was first recognised by Nguyen (1997).

Similarly, the orientation and reverse shear sense of the low displacement, ore-hosting structures on the western side of the Playa Fault for more than 5 km NW of the jog (i.e. the Victory–Revenge area), are also interpreted as

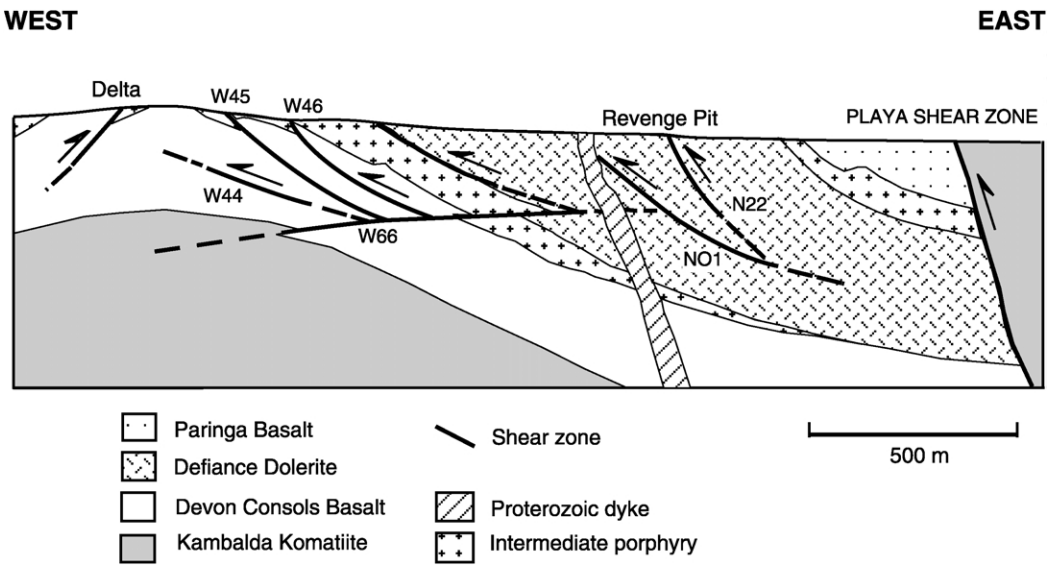

Fig. 6. Simplified E–W cross-section of the Revenge mine area. Gold deposits (numbered) are hosted in conjugate thrusts just west of the Playa Fault (after Nguyen et al., 1998).

contractional structures whose formation is kinematically-related to predominantly sinistral slip on the Playa Fault during D_3. Accordingly, the gold deposits in the Orchin to Revenge areas are interpreted to have formed in a low displacement contractional damage zone generated by strain accommodation around the Victory jog. As the Playa Fault was inclined to the maximum principal stress during D_3 by approximately 50°, it was not optimally oriented for E–W shortening during D_3. This is consistent with the structure having initiated during D_2 and being reactivated during D_3.

North-west of the Revenge area, several gold deposits and prospects occur within the Playa Fault, or west of this structure (Fig. 4). The Delta and Santa Ana deposits are localised in NW-trending fault zones west of the Playa Fault. The Formidable and Belle Isle prospects, and the

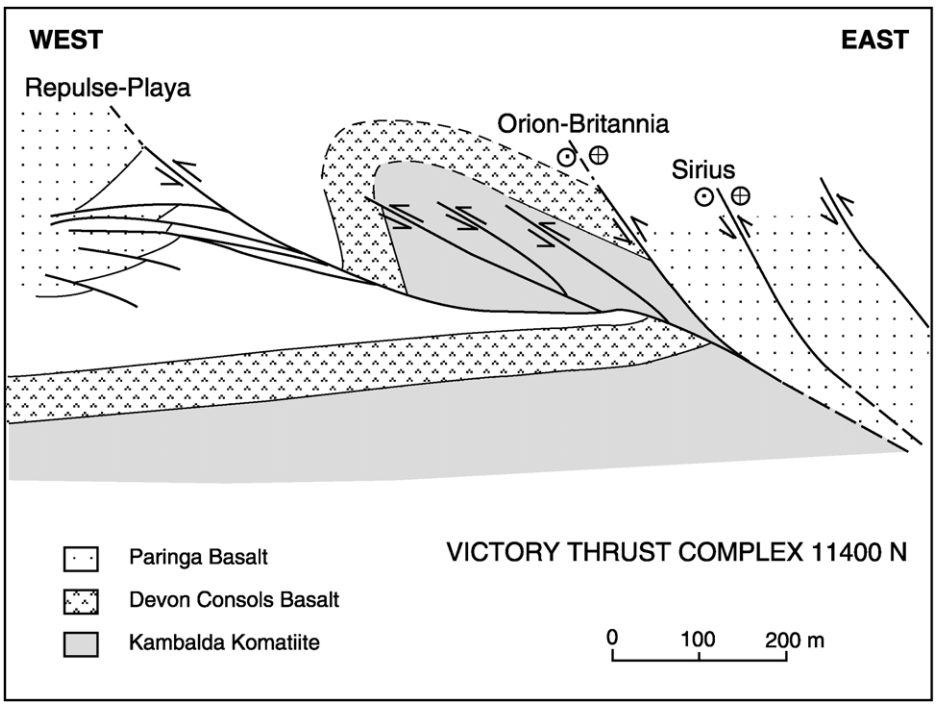

Fig. 7. Simplified E–W cross-section of the Victory thrust complex. All faults in the thrust system are associated with gold mineralisation (modified after St Ives Gold Mining Company data and authors' work). Positions of numerous felsic to intermediate intrusives are omitted for clarity.

Redoubtable and Intrepide deposits occur within the Playa Fault, or strands of this structure. The Minotaur, Mars and Agamemnon deposits are associated with shear zones that are likely to be link structures between the Playa Fault and the Delta Fault north of the Delta deposit. The Argo and Junction deposits are spatially separated from the other St Ives deposits and occur south of the Victory jog and west of the BLF. Argo occurs within a moderately west-dipping, brittle–ductile, reverse shear zone. The Junction deposit occurs along an east-dipping, NNW-trending, reverse/sinistral shear zone. Maximum displacement on these latter structures is between 50 and 100 m.

Alteration assemblages formed during gold mineralisation in D_3 shear zones indicate deformation at temperatures of approximately 400 °C (Clark et al., 1989). Pressures are more poorly-constrained, but are interpreted to have been up to 300 MPa (Clark et al., 1989). U–Pb geochronology on rutile, monazite and xenotime in ore assemblages indicate that gold mineralisation during D_3 occurred at approximately 2.63 Ga (Clark et al., 1989; Nguyen, 1997; Nguyen et al., 1998).

Displacement on ore-hosting structures in the St Ives goldfield involved both ductile and brittle processes. Hydrothermal alteration and associated gold mineralisation was synchronous with deformation along the ore-hosting network of shear zones. For example, at the Revenge mine, mineralised shears exhibit evidence for early brittle slip events and brecciation, followed by ductile shearing and foliation development during progressive potassic and carbonate alteration, gold precipitation and vein formation (Nguyen et al., 1998). In many deposits, ductile shearing was punctuated by repeated brittle slip events, which produced breccias and shear veins (Fig. 8), especially in jogs and dilatant bends in shear zones.

The widespread development of subhorizontal extension vein arrays adjacent to the reverse shears which host mineralisation (Fig. 8) indicates that the fluids responsible for mineralisation and hydrothermal alteration were repeatedly at supralithostatic pressures during deformation on lode-hosting structures. Vein development in gold lodes is most intense in much of the Victory thrust complex, as well as in the Junction and Revenge deposits. Veining is much less abundant north and north-west of the Revenge deposits in the Minotaur–Redoubtable–Santa Ana area, and also to the west and south-west of the Victory thrust complex in the North Orchin and Argo deposits. High fluid fluxes associated with near-lithostatic pore fluid pressures are a key factor driving growth of low displacement faults, fractures and shear zones which host the Au deposits at St Ives (Nguyen et al., 1998; Cox, 1999; Cox et al., 2001).

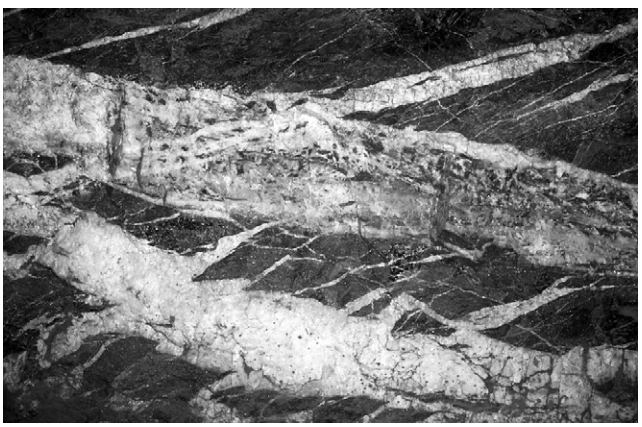

Fig. 8. Fault-related vein system forming part of the Defiance lode system in the footwall of the Playa Fault, Victory thrust complex. Quartz veins dipping to the right are fault-fill gold lodes in dilatant thrusts. They are associated with gently left-dipping extension veins. Shear sense is top to the left. Host rock is Defiance Dolerite.

4. Application of stress transfer modelling in the St Ives goldfield

As the location of rupture arrest sites is a key factor controlling the distribution of major co-seismic static stress changes and aftershock activity, useful predictive modelling, using this approach, requires the identification of structural sites favouring repeated rupture arrest. On the basis that many earthquake ruptures terminate at fault jogs (e.g. Sibson, 1990), we test the hypothesis that the major contractional jog at the Victory thrust complex was a significant rupture arrest site for repeated ruptures propagating along the Boulder–Lefroy–Playa fault system (Fig. 5). Accordingly, we use Coulomb stress transfer modelling to examine static stress changes in response to rupture arrest at this site, and to determine whether the distribution of gold-hosting structures matches modelled domains of positive ΔCFS.

Most of the gold-hosting structures have maximum lengths of about 1 km. Faults of these dimensions usually rupture with earthquakes having maximum moment magnitudes of approximately 3–4.5 (Wells and Coppersmith, 1994). Aftershocks of this magnitude are very typically driven by mainshocks with magnitudes of six or more. Accordingly, the modelling specifically explores static stress changes arising from a rupture with a maximum displacement of 1 m along a 30-km-long rupture segment on the Boulder–Lefroy–Playa fault (BLPF) system. This is approximately equivalent to rupture events with a moment magnitude of 6.0–6.5 (Wells and Coppersmith, 1994).

As the Coulomb 1.0 modelling technique calculates static stress changes associated with slip on planar fault segments, the 30-km-long rupture patch on the BLPF has been modelled as four vertically dipping fault segments (numbered 1–4 from the NW to SE), which closely match the surface trace of the fault (Fig. 9a). The central two segments (2 and 3) have a modelled sinistral slip of 1 m and the outer two segments have a slip of 0.5 m. The NW end of the rupture patch is terminated at the Victory jog. A lack of geological information in the SE part of the modelled region

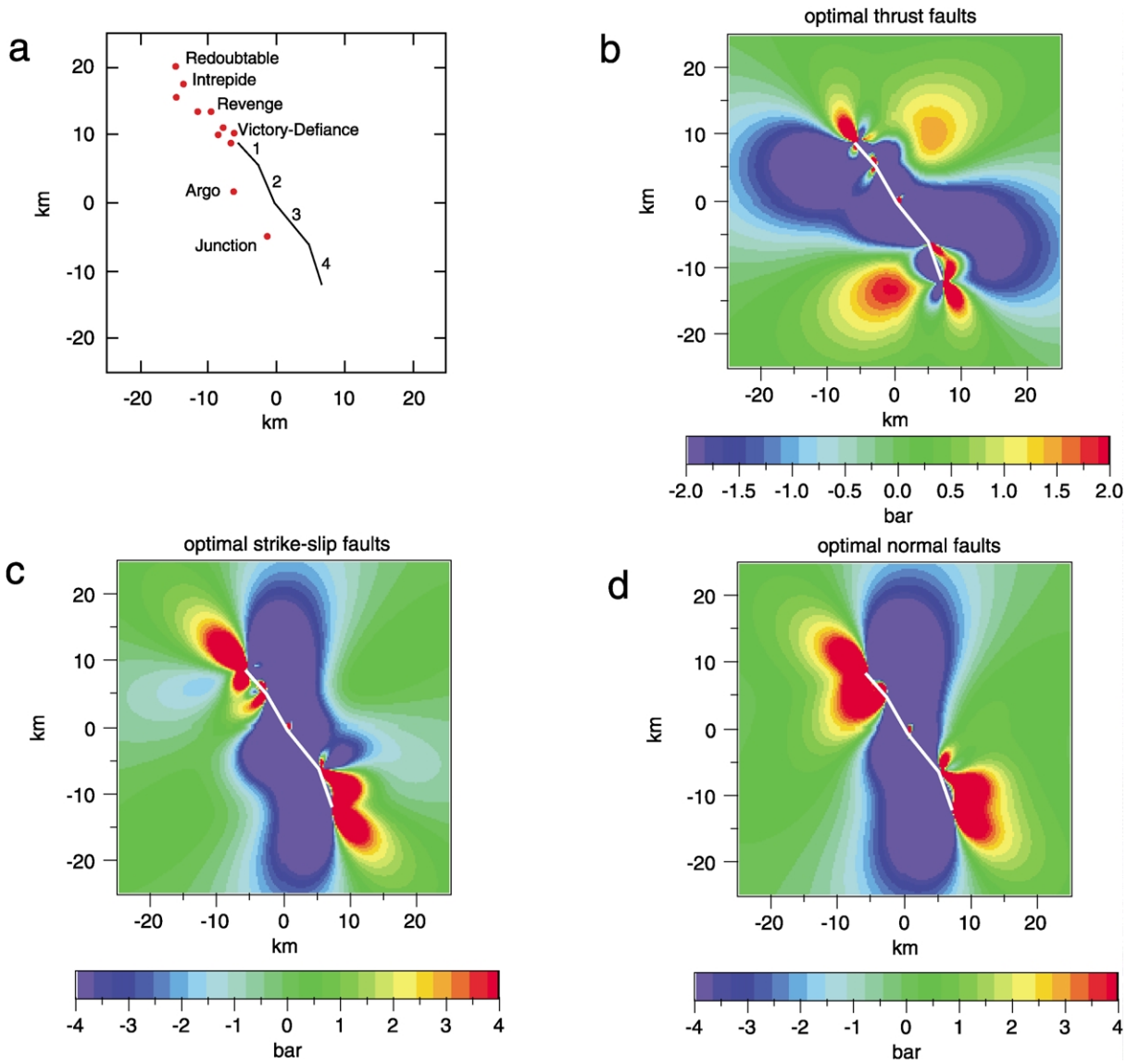

Fig. 9. (a) Map illustrating the area covered by 3-D finite element modelling using Coulomb 1.0. Position of the modelled rupture surface on the Boulder–Lefroy–Playa Fault is indicated, together with the location of some major gold deposits in the St Ives goldfield. The modelled rupture surface on the Boulder–Lefroy–Playa Fault has its north-western termination at the Victory jog and is indicated by the black line. Fault segment numbers are indicated. Modelling is performed with an E–W maximum principal stress. The stress difference at the depth of deposit formation is set at 40 MPa. Apparent friction is 0.4. (b) Distribution of Coulomb failure stress change around the Boulder–Lefroy–Playa fault system for optimally-oriented thrust faults. (c) Distribution of Coulomb failure stress change for optimally-oriented strike-slip faults. (d) Distribution of Coulomb failure stress change for optimally-oriented normal faults.

currently precludes identification of potential rupture arrest sites in that area. As the main objective of the modelling is to analyse static stress changes in the St Ives area, the SE end of the rupture patch is arbitrarily terminated 30 km SE of the Victory jog.

Changes in CFS were calculated over a crustal depth between 3 and 20 km, and over an area of 50 km × 50 km, centred on the middle of the modelled rupture surface (Fig. 9a). The stress changes have been calculated on a 200 m × 200 m grid, using an apparent friction coefficient of 0.4. This corresponds to a friction coefficient of 0.75 and Skempton's coefficient (B) of 0.47.

The modelled maximum principal stress is oriented E–W, consistent with that indicated by the geometry and kinematics of lode-hosting faults and their vein arrays. The far-field intermediate principal stress is modelled as vertical. The Poisson's ratio is set at 0.25 and the elastic modulus is 8×10^5 MPa.

The modelled results for static stress changes on optimally-oriented strike-slip, thrust and normal aftershock faults are illustrated in a depth slice at 12 km in Fig. 9b–d. This depth corresponds approximately to the presently exposed structural level in the St Ives goldfield. In the modelled volume, reverse aftershock faults are approximately N–S-trending and gently to moderately east- or west-dipping; normal aftershocks occur on approximately

E–W-trending structures which are moderately to steeply north- or south-dipping; strike-slip aftershocks occur on steeply-dipping, N–W-trending sinistral faults, or N–E-trending dextral faults.

The modelling indicates that, for a sinistral mainshock rupture propagating northwards along the BLFP and arresting at the Victory jog, optimally-oriented reverse, strike-slip and normal faults located in an elongate lobe of positive ΔCFS north-west of the Victory jog all have stress states that are closer to failure as a result of co-seismic stress transfer. A strong correlation exists between this modelled lobe of increased Coulomb failure stress and the distribution of most known gold deposits and prospects in the St Ives goldfield. Coulomb failure stress is increased in a domain that extends for up to 10 km north-west of the Victory jog for all fault types. The static stress change is smaller for thrust faults than for strike-slip faults and normal faults. Also, the lobe of positive ΔCFS has a larger area for strike-slip and normal structures than for thrust faults. This is consistent with gold-hosting reverse structures being well-developed close to the Victory jog (Victory–Revenge area), whereas several structures hosting lodes further NW have significant strike-slip components (e.g. Santa Ana). Rupture arrest at the Victory jog also increases proximity of stress states to failure for sinistral slip on the Playa Fault and its strands NW of the jog. So deposits and prospects on the Playa Fault in this area (e.g. Belle Isle, Formidable, Intrepide and Redoubtable) also have locations consistent with stress triggering due to mainshock arrest at the Victory jog. For thrust faults, there is also a lobe of increased proximity to failure about 10 km north-east of the Victory jog (Fig. 9b). This area is currently unexplored.

Although the major Argo deposit (SW of the Victory jog) is hosted by a N–S-trending, moderately west-dipping reverse shear zone, it and a cluster of nearby prospects, are not within a domain of significant positive ΔCFS for thrust aftershocks in the pure strike-slip stress transfer model of the BLPF (Fig. 10a and b). There is a very small nearby lobe of weak positive ΔCFS just to the east; this lobe is generated by the presence of a bend in the BLPF to the east, linking modelled segments 1 and 2 of the BLPF. However, a mixed component of sinistral-oblique slip on the BLPF in modelled segment 2 would be more realistic if slip on segment 1 is purely sinistral. This change in slip vector causes the lobe of positive ΔCFS at the segment junction to strengthen and expand to encompass the Argo area (Fig. 10c). This same area is also a lobe of positive ΔCFS for strike-slip and normal aftershocks in the pure strike-slip model of slip on the BLPF (Fig. 10c and d).

The major Junction gold deposit (20 tonnes Au) formed in a north-west-trending oblique reverse-sinistral shear zone 4 km south-west of the BLPF (Fig. 4). This deposit lies well outside the modelled areas of increased failure proximity due to rupture arrest at the Victory jog. Accordingly, if the Junction deposit has an aftershock origin related to slip on the BLPF, its position is unlikely

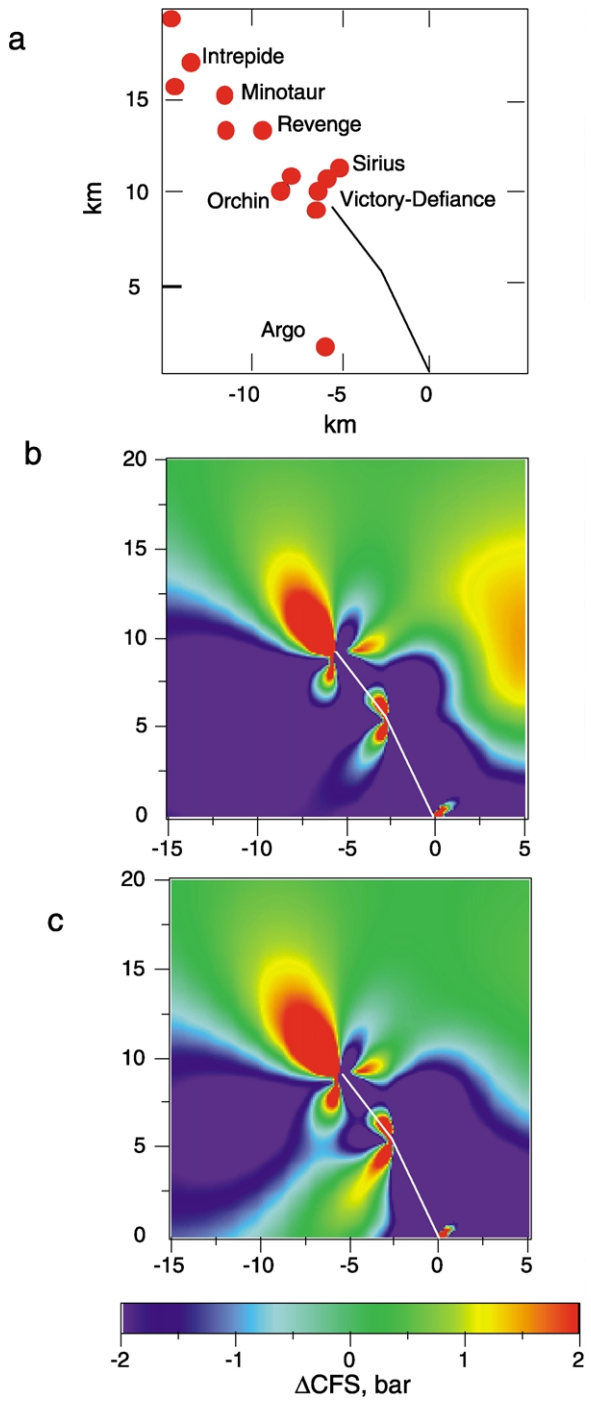

Fig. 10. (a) Detail of distribution of gold deposits and modelled rupture surface location in the Victory–Argo area. (b) Changes in Coulomb failure stress for optimally-oriented reverse faults in the pure strike-slip model. (c) Changes in Coulomb failure stress for optimally-oriented reverse aftershock faults for a model in which fault segment 2 has 1 m of sinistral strike slip and 1.5 m of west-side-up slip.

to have been influenced by static stress change associated with rupture arrest at the Victory jog. Instead, given the distribution of static stress change lobes for production of reverse aftershocks in sinistral driving fault systems, the position of the Junction deposit could be related to

southwards propagating sinistral slip events arresting near the bend between segments 3 and 4 of our modelled BLPF (Fig. 9a). Alternatively, its development could be related to co-seismic stress change associated with slip on other high displacement faults, such as the Merougil Fault, which is located 7 km west of Junction, or as yet unidentified faults in this region of very poor outcrop.

Lobes of positive ΔCFS are also developed at the SE end of the modelled strike-slip rupture patch (Fig. 9). These lobes are asymmetrically distributed relative to the lobes in the St Ives goldfield at the NW end of the modelled rupture patch. The detailed geometry of the lobes reflects effects of the modelled fault bend between segments 3 and 4. Although the rupture arrest site in this part of the model has been arbitrarily chosen, the modelling illustrates the point that domains of increased proximity to failure develop in three dimensions all around the perimeter of a rupture patch. Whether or not a major aftershock network develops will depend on whether ruptures consistently arrest at particular locations (i.e. characteristic earthquakes repeatedly arresting at a geometric asperity such as a bend or jog). Whether the aftershock network becomes mineralised will depend on its capacity to tap into appropriate fluid reservoirs.

5. Discussion

5.1. General aspects

Mesothermal gold deposits tend to develop predominantly within low displacement faults or shear zones adjacent to much higher displacement structures In addition, they tend to occur in localised clusters within crustal-scale shear systems. The St Ives goldfield provides a particularly good example of this. Other clusters of deposits, which are spatially associated with the BLF, occur 30 km to the north of St Ives in the New Celebration area, 80 km to the north in the Kalgoorlie area, and 120 km to the north in the Paddington region.

In the St Ives goldfield the cluster of mineralisation is developed predominantly in:

1. An imbricate thrust fan within a contractional jog (Victory jog) in a sinistral to sinistral-oblique shear system (Fig. 7)
2. Arrays of approximately N–S-trending, low displacement reverse shears in a belt up to 2 km wide and 10 km long, immediately west of the Playa Fault and NW of the Victory jog (Figs. 4 and 5)
3. NW-trending, mixed reverse to strike-slip faults up to several kilometres west of the Playa Fault
4. Vein networks in competent rock units within and adjacent to the Playa Fault
5. Reverse to reverse-sinistral shear zones south of the Victory Complex (Argo and Junction deposits)

On the basis of the correlation between modelled sites of positive ΔCFS and the distribution of known gold mineralisation in the St Ives goldfield, it is proposed that the generation of low displacement, gold-hosting structures has been influenced by stress transfer associated with arrest, at the Victory jog, of large, NW-propagating slip events on the Boulder–Lefroy–Playa fault system.

A key factor controlling the distribution of the gold-hosting faults and shear zones is interpreted to be the development of the kilometre-scale contractional jog on the strike-slip Playa Fault, just NW of where it splays from the larger BLF. Strain accommodation around this structure is interpreted to have established a broad zone of contractional deformation extending for 5–10 km NW of the jog. The imbricate thrusts and associated vein-hosting fracture arrays in the Victory jog provided high fracture connectivity and high permeability through the jog, causing extreme localisation of fluid flow. Arrays of low displacement, gold-hosting faults and shear zones up to 10 km north-west of the jog, and to a lesser extent, to the south of the jog, are kinematically related to shortening in the jog, and are interpreted to have developed in response to localised stress changes generating a transpressional regime around the jog. Growth of this low displacement contractional fault network has controlled ore fluid pathways and apparently tapped mineralising fluids from the jog and possibly deeper levels of the Playa Fault. The damage network will have been most permeable immediately after slip events within the network. Hydrothermal, self-sealing, between slip events is expected to have controlled episodic flow, fluid pressure cycling and fault-valve behaviour in the system.

It is concluded that clustering of mesothermal gold deposits may be controlled by the development of barriers to repeated rupture propagation on crustal-scale fault systems, which are active when gold-producing hydrothermal systems are being generated.

The association between gold deposits and low displacement faults and shear zones indicates that fluid redistribution after large slip events was localised on aftershock damage networks. The Victory jog is a zone of particularly high fault/vein density. Immediately after major slip events on the BLPF the jog is likely to have had substantially higher permeability than the rest of the modelled high displacement mainshock rupture surface. Therefore it will have localised most of the post-slip fluid discharge. Jogs within strike-slip fault systems have strong vertical connectivity (Cox et al., 2001) and can provide the best potential for tapping deeper crustal fluid reservoirs, or facilitating mixing between deep and shallow crustal reservoirs during the genesis of lode gold systems.

The stress transfer modelling and the behaviour of modern seismogenic systems both highlight the point that aftershock ruptures can involve strike-slip, thrust and

normal faults or shear zones, regardless of slip sense on the larger driving structures. Although substantial gold mineralisation at St Ives is associated with reverse and strike-slip structures, major mineralisation has not yet been recognised on normal faults or shear zones in the St Ives area. In the regional stress field prevailing during D_3 mineralisation, optimally-oriented normal faults would be E–W-trending. There are numerous very small (< 1 m slip), E–W-trending shear zones in the North Orchin area which have normal shear sense and which are associated with biotite alteration and elevated, but sub-economic, gold grades. Similarly at Intrepide there is a south-dipping normal fault and associated gold-bearing quartz fault-fill veins and steep extension veins. Accordingly there is potential for larger, E–W-trending, mineralised normal faults or shears to form part of the aftershock array adjacent to the Boulder–Lefroy–Playa fault system. The relative sizes of the positive ΔCFS lobes favouring thrust, strike-slip and normal aftershocks indicate that although gold-hosting structures are predominantly thrust structures near the Victory jog, strike-slip and normal faults and shear zones might be more abundant further to the NW. South and south-west of the jog, the modelling for pure strike-slip mainshocks indicates that the potential for strike-slip and normal aftershock structures is greater than for reverse faults and shears.

5.2. Slip processes

There is clear evidence of repeated, and probably seismogenic, brittle shear failure on many of the low displacement, lode-hosting structures. Hydrothermal sealing of faults and associated breccias, cataclasites and macroscopic fracture arrays occurred between slip events. However, aseismic creep has also occurred between brittle slip events and produced foliations in the hydrothermally altered wall-rocks immediately adjacent to faults.

It is unclear whether the high displacement driving structure (the Boulder–Lefroy–Playa Fault) was necessarily seismogenic at the depth of formation of the St Ives gold system. The inferred temperature and depth of the system during D_3 places it near the base of the seismogenic regime for continental crust. The presence of strongly foliated fault-rocks in the limited exposure and drill-core intersection of the BLP fault indicates substantial displacement was accommodated by ductile creep. However, this does not preclude episodic seismogenic slip and co-seismic stress transfer. Nevertheless, even below the base of the continental seismogenic regime, episodes of aseismic creep, which are geometrically impeded from propagating past the Victory jog, will result in stress transfer comparable with that associated with purely seismogenic slip, but on a slower timescale.

5.3. Role of fluid pressures in nucleating aftershocks

Although the spatial distribution of aftershocks around mainshock ruptures is generally closely related to static stress changes brought about by mainshock slip (King et al., 1994), changes in aftershock activity also may be influenced by post-seismic fluid pressure changes. For example, it has been argued that decay in aftershock activity with time, as well as time-dependent shifts in aftershock locations, can be influenced by pore fluid redistribution and associated changes in pore fluid pressures and effective stress states after mainshocks (Nur and Booker, 1972; Harris, 1998).

The stress transfer modelling in this study has explicitly related changes in fluid pressure to poroelastic responses to co-seismic changes in stress state. However, there are also likely to be time-dependent changes in fluid pressures associated with post-seismic fluid redistribution around slipped and permeable faults (Cocco and Rice, 2002; Harris, 1998). The pervasive hydrothermal alteration and vein development in the gold-hosting structures at St Ives indicates that high fluid fluxes were associated with the operation of the shear network. The known distribution of mineralisation and vein development indicates that the most intense and volumetrically significant alteration, gold mineralisation and fluid flux were likely centred on the Victory jog. A general decrease in vein abundance in mineralised shears remote from the Victory jog (e.g. Santa Ana, Minotaur, Intrepide, Redoubtable in the NW) may indicate an overall decrease in maximum pore fluid pressures (and accordingly fluid flux?) away from the jog. This is consistent with the high density of low displacement faults and vein arrays in the jog providing an episodically-permeable, vertically well-connected fluid pathway each time it was reactivated by a major slip event being arrested at the Victory jog (Fig. 11).

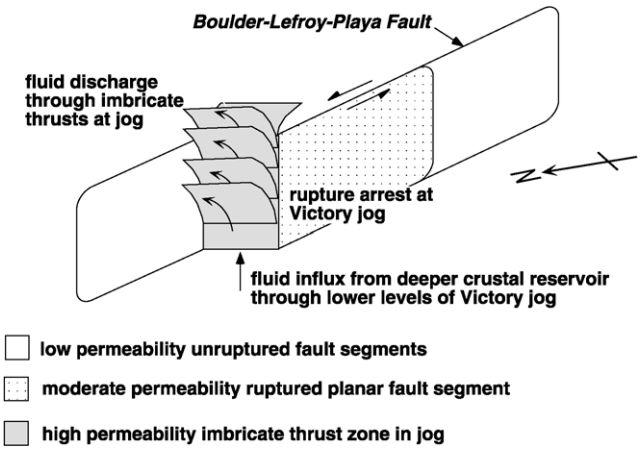

Fig. 11. 3-D schematic of fluid transport in the Boulder–Lefroy–Playa Fault after a rupture event. Highest bulk permeability is localised within the damage zone at the contractional jog (Victory thrust complex) rupture arrest site. This leads to high fluid flux and fluid discharge from the jog domain immediately after rupture. Progressive infiltration of fluids out from the jog and into the surrounding rock volume after the mainshock builds up supralithostatic fluid pressures and acts together with co-seismic Coulomb stress changes to drive aftershocks on low displacement faults. Permeability enhancement in low displacement structures subsequent to each aftershock drives transiently high fluid flux and gold deposition in these structures.

The jog was characterised by the prevalence of near-lithostatic fluid pressure conditions during vein formation and gold deposition. This requires that the thrust network was capped by a low permeability domain (fault seals?) that inhibited upwards drainage into a shallow crustal, hydrostatic fluid-pressured regime after slip events. The alteration envelopes around lode deposits indicate that fluids discharged from faults into the surrounding, initially low permeability rock mass. It is likely that after each slip event that arrested at the Victory jog, fluid discharge from the jog led to gradual fluid pressure increase in an expanding domain around the jog, and contributed to fluid-driven failure in the low displacement faults in that area. With progressively increasing pore fluid pressures, fluid-driven failure must have propagated laterally away from the Victory jog, preferentially nucleating aftershocks in those domains where mainshock stress transfer had caused positive changes in the Coulomb failure stress. This scenario is similar to that examined by Harris (1998) and Bosl and Nur (2002) for time-dependent propagation of aftershocks outwards from the 1992 Landers rupture during post-seismic fluid redistribution.

Successive events of fluid migration away from the Victory jog are interpreted to have assisted repeated reactivation of the aftershock network for up to 10 km away from the jog, and driven incremental growth of gold deposits after each major slip event. Development of the gold system is likely to have been terminated either by draining of the fluid reservoir responsible for the hydrothermal system, or by rupture arrest ceasing to occur at the Victory jog.

5.4. Implications for exploration and the origin of mesothermal gold deposits

The concept that many low displacement faults and shear zones, which host mesothermal gold deposits, may be aftershock structures has important implications for the development of novel, yet relatively straightforward conceptual approaches to understanding the distribution of mesothermal gold systems within crustal-scale fault systems. If, as in the present study, barriers to rupture propagation, such as jogs, bends or fault terminations, can be recognised in gold-producing terrains, then stress transfer modelling can be used as an area selection tool during gold exploration.

Significantly for exploration targeting, the stress transfer modelling indicates that domains of positive ΔCFS occur up to 15 km away from the mainshock arrest site. The modelling therefore indicates that the area in which aftershock-related gold deposits may develop is much larger than the immediate vicinity of flow-localising jogs or bends on large displacement structures. Clustering of deposits, to produce areally extensive goldfields, is likely to be favoured by the presence of long-lived jogs or bends on high displacement faults. These geometric asperities are a major cause of rupture arrest during mainshocks. Note, however, that as high displacement faults accumulate slip, the frequency of fault irregularities such as jogs decreases (Wesnousky, 1988). This 'fault smoothing' with time (Sibson, 2001) means that jogs can eventually be short-cut, become inactive, and no longer serve to arrest major ruptures. This process could terminate the formation of goldfields.

The technique can be applied in 'greenfields' environments to help target gold potential in domains of tens to hundreds of square kilometres in area. In addition, it can be applied in mature goldfields to help locate new prospective areas. For the St Ives region, the stress transfer modelling: (1) indicates the presence of lobes of positive ΔCFS where gold potential had not been assessed; (2) highlights that exploration has not tested large areas of the positive ΔCFS lobes which are currently known to host gold mineralisation; (3) predicts potential for gold mineralisation in E–W-trending faults and shear zones; and (4) indicates the possibility of other rupture arrest points developing elsewhere on the BLF, or in adjacent high displacement faults. Furthermore, stress transfer modelling also has potential application at smaller scales, for mine-scale extensional exploration. Large aftershocks can themselves generate small aftershocks around their rupture zone. Accordingly, modelling of stress changes associated with slip on known, kilometre-scale gold-hosting structures could predict distribution of smaller-scale, mineralised splays around the margins of these structures, or around jogs and bends in these structures.

Future modelling and further case studies will explore in more detail how changes in parameters such as stress difference, slip magnitude, stress orientations, apparent friction coefficient and elastic modulus affect the results. Initial work indicates that modest changes to these parameters do not severely change the distribution of lobes of CFS increase and decrease, only their magnitudes and relative areas. However, very low far-field stress differences can result in substantially increased ΔCFS in domains along the mainshock rupture surface. Furthermore, it must be borne in mind that aftershock distribution is unlikely to be controlled entirely by co-seismic static stress transfer. Particularly as mesothermal gold deposits develop in high fluid flux hydrothermal systems, the distribution of aftershock structures will also be modulated by changes in fluid pressures, and hence effective stress states, due to transitory fluid redistribution around shear systems after large slip events. Accordingly, fluid invasion of slipped fault segments, and consequent fluid-driven failure following major slip events, may act together with mainshock-related stress redistribution in localising aftershock activity, fluid flow and gold mineralisation in mesothermal gold systems.

The present modelling assumes an elastically homogeneous and isotropic crust. Mechanical heterogeneity associated with lithological contrasts is also likely to modulate the distribution of Coulomb stress changes,

producing second-order effects, additional to the first-order effects modelled herein. Despite this, stress transfer modelling in modern seismogenic fault systems produces very good correlation between aftershock activity and changes in Coulomb failure stress.

Understanding of how proximity to failure is influenced by slip processes and fluid redistribution in fracture-controlled hydrothermal systems will be of use for understanding the distribution and genesis of mesothermal gold systems not just in Archaean, but also in younger terranes where fault-hosted mesothermal gold systems are well-developed. Stress transfer modelling may also have application to other epigenetic mineralisation styles whose development is also influenced by growth of fault and fracture systems (e.g. some epithermal systems, magmatic-related systems, and Carlin systems).

5.5. Comparison with other structural approaches to ore targeting

A classical structural approach to ore targeting in fracture-controlled ore environments focuses on the role of jogs, especially dilatant jogs, for localising high flux fluid flow and ore deposition in fault zones (e.g. Sibson, 1986; Cox, 1999). In this approach, the jog itself is the ore target and the surrounding region is essentially ignored. Stress transfer modelling provides a conceptual approach to ore deposit targeting that is distinct from this basic type of structural targeting because it focuses on the role of major irregularities (bends and jogs) in high displacement faults as mainshock rupture arrest sites, which drive the formation of areally extensive aftershock fracture networks. Stress transfer modelling not only targets major bends and jogs (both dilational and contractional) on high displacement structures, but also the low displacement, ore-hosting fracture networks that may extend for many kilometres away from the jogs.

Other numerical modelling approaches, using distinct element or finite element techniques, have a very different conceptual basis from that of stress transfer modelling. For example, the 'stress mapping' technique of Holyland and Ojala (1997) uses 2-D and 3-D modelling of low strain elastic-frictional deformation of mechanically heterogenous crust to determine where the most dilatant sites might occur. The technique assumes that ore fluids will migrate to, or pass through, these sites. In a related approach, Sanderson and Zhang (1999) have modelled the elastic–frictional reactivation of pre-existing fracture networks. This approach tests how the apertures of fractures, at various orientations to the applied stress field, changes with deformation. Because of the cube law relationship between fracture aperture and flow rates, most fluid flow in a reactivated, dilatant fracture network becomes localised along the highest aperture fractures.

6. Conclusions

Low displacement faults which localise fluid flow and host mesothermal gold deposits in the St Ives goldfield of the Archaean Yilgarn Craton are interpreted as aftershock structures formed around high displacement faults and shear zones during repeated, major, seismogenic rupture or aseismic creep events. Clustering of the gold deposits and localisation of high flux fluid flow required to form them has been controlled by the development of the kilometre-scale contractional Victory jog within the Boulder–Lefroy fault system at St Ives.

The application of Coulomb stress transfer modelling to analyse the distribution of gold deposits in the St Ives goldfield indicates that their distribution can be related to repeated, major slip events on part of the Boulder–Lefroy fault system being arrested at the Victory jog. Modelled Coulomb failure stress changes define a domain of increased Coulomb failure stress (and higher aftershock probability) closely coincident with the location of the St Ives goldfield. The modelling also points to other areas of positive ΔCFS around the Boulder–Lefroy fault system in the region; these represent new targets for gold exploration. Accordingly, modelling of co-seismic static stress change may provide a powerful tool to assist area selection in exploration programs targeting mesothermal gold systems. The technique will also have application to other fault-related epigenetic deposit styles. Clustering of deposits hosted by aftershock fracture networks is favoured by the presence of major, long-lived jogs or bends that can repeatedly arrest ruptures propagating along high displacement faults.

Acknowledgements

WMC Resources Ltd St Ives Gold Operations and St Ives Gold Mining Company Ltd (a division of Gold Fields Ltd) are thanked for financial and logistical support. Both companies provided open access to mine sites and company data over several years. Our research at St Ives was facilitated by K. Hein, W. Stone and W. Morrison. Our understanding of the regional and deposit geology has benefited from discussions with numerous geoscientists at St Ives. We particularly acknowledge the work of P. Nguyen, which formed the foundation for this study, and the work of the many St Ives geoscientists on whose work Figs. 4 and 5 are partly based. Extensive discussions with R. Sibson and S. Micklethwaite are greatly appreciated. USGS and S. Toda are thanked for making the Coulomb modelling package freely available. The later parts of this study were supported by an Australian Research Council Linkage Grant to Cox. Ruming was supported by an Australian Postgraduate Research Award (Industry). Reviews by J. Ridley and an anonymous reviewer were particularly valuable, as were comments by Special Volume guest editor J. Vearncombe.

References

Aki, K., 1984. Asperities, barriers, characteristic earthquakes and strong motion prediction. Journal of Geophysical Research 89, 5867–5872.

Beroza, G.C., Zoback, M.D., 1993. Mechanism diversity of the Loma Prieta aftershocks and mechanisms for mainshock–aftershock interaction. Science 259, 210–213.

Bosl, W.J., Nur, A., 2002. Aftershocks and pore fluid diffusion following the 1992 Landers earthquake. Journal of Geophysical Research 107, 2366ESE17-1–ESE17-9, DOI: 10.1029/2001JB000155.

Boullier, A.-M., Robert, F., 1992. Palaeoseismic events recorded in Archaean gold–quartz vein networks, Val d'Or, Quebec, Canada. Journal of Structural Geology 14, 162–177.

Clark, M.E., Carmichael, M.D., Hodgson, C.J., Fu, M., 1989. Wall-rock alteration, Victory Gold Mine, Kambalda, Western Australia: Processes and P-T-XCO2 conditions of metasomatism. In: Keays, R.R., Ramsay, W.R.H., Groves, D.I. (Eds.), The Geology of Gold Deposits: The Perspective in 1988. Economic Geology Monograph 6, pp. 445–459.

Clout, J.M.F., Cleghorn, J.H., Eaton, P.C., 1990. Geology of the Kalgoorlie goldfield. In: Hughes, F.E. (Ed.), Geology of the Mineral Deposits of Australia and Papua New Guinea.Australasian Institute of Mining & Metallurgy, Monograph Series, 14, pp. 411–431.

Cocco, M., Rice, J.R., 2002. Pore pressure and poroelasticity effects in Coulomb stress analysis of earthquake interactions. Journal of Geophysical Research, 107(ESE 2, 1–17).

Cox, S.F., 1995. Faulting processes at high fluid pressures: an example of fault-valve behavior from the Waltie Gully Fault, Victoria, Australia. Journal of Geophysical Research 100, 841–859.

Cox, S.F., 1999. Deformational controls on the dynamics of fluid flow in mesothermal gold systems. In: McCaffrey, K.J.W., Lonergan, L., Wilkinson, J.J. (Eds.) Fractures, Fluid Flow and Mineralisation. Geological Society of London, Special Publication 155, pp. 123–140.

Cox, S.F., Wall, V.J., Etheridge, M.A., Potter, T.F., 1991. Deformational and metamorphic processes in the formation of mesothermal vein-hosted gold deposits—examples from the Lachlan fold belt in central Victoria, Australia. Ore Geology Reviews 6, 391–423.

Cox, S.F., Knackstedt, M.A., Braun, J., 2001. Principles of structural control on permeability and fluid flow in hydrothermal systems. Society of Economic Geologists Reviews 14, 1–24.

Foster, R.P., 1989. Archaean gold mineralisation in Zimbabwe: implications for metallogenesis and exploration. In: Keays, R.R., Ramsay, R.W.H., Groves, D.I. (Eds.), The Geology of Gold Deposits: The Perspective in 1988. Economic Geology Monograph 6, pp. 54–70.

Goldfarb, R.J., Groves, D.I., Gardoll, S., 2001. Orogenic gold and geologic time: a global synthesis. Ore Geology Reviews 18, 1–75.

Groves, D.I., Barley, M.E., Ho, S.E., 1989. Nature, genesis and tectonic setting of mesothermal gold mineralisation in the Yilgarn block, Western Australia. In: Keays, R.R., Ramsay, R.W.H., Groves, D.I. (Eds.), The Geology of Gold Deposits: The Perspective in 1988. Economic Geology Monograph, 6, pp. 71–85.

Groves, D.I., Ridley, J.R., Bloem, E.M.J., Gebre-Meriam, M., Hagemann, S.G., Hronsky, J.M.A., Knight, J.T., McNaughton, N.J., Ojala, J., Vielreicher, R.M., McCuaig, T.C., Holyland, P.W., 1995. Lode-gold deposits of the Yilgarn Block: products of late-Archaean crustal-scale overpressured hydrothermal systems. In: Coward, M.P., Ries, A.C. (Eds.), Early Precambrian Processes. Geological Society of London, Special Publication 95, pp. 155–172.

Harris, R.A., 1998. Introduction to special section: stress triggers, stress shadows and implications for seismic hazard. Journal of Geophysical Research 103, 24347–24358.

Harris, R.A., Archuleta, R.J., Day, S.M., 1991. Fault steps and the dynamic rupture process: 2-D numerical simulations of a spontaneously propagating shear fracture. Geophysical Research Letters 18, 893–896.

Holyland, P.W., Ojala, V.J., 1997. Computer-aided structural targeting in mineral exploration: two- and three-dimensional stress mapping. Australian Journal of Earth Sciences 44, 421–432.

Jaeger, J.C., Cook, N.G.W., 1979. Fundamentals of Rock Mechanics, 3rd ed, Chapman and Hall, London.

King, G.C., 1986. Speculations on the geometry of the initiation and termination processes of earthquake rupture and its relation to morphology and geologic structure. Pure and Applied Geophysics 124, 567–585.

King, G.C., Stein, R.S., Lin, J., 1994. Static stress changes and the triggering of earthquakes. Bulletin of the Seismological Society of America 84, 935–953.

Knopf, A., 1929. The Mother Lode System of California. United States Geological Survey Professional Paper 157, 88pp.

McKeag, S.A., Craw, D., 1989. Contrasting fluids in gold-bearing quartz vein systems formed progressively in a rising metamorphic belt: Otago Schist, New Zealand. Economic Geology 84, 22–33.

Nguyen, T.P., 1997. Structural controls on gold mineralisation at the Revenge Mine and its tectonic setting in the Lake Lefroy area, Kambalda, Western Australia. PhD thesis, University of Western Australia.

Nguyen, P.T., Cox, S.F., Powell, C.McA., Harris, L., 1998. Fault-valve behaviour in optimally-oriented shear zones at Revenge gold mine, Kambalda, Western Australia. Journal of Structural Geology 20, 1625–1640.

Nur, A., Booker, J.R., 1972. Aftershocks controlled by pore fluid flow? Science 175, 885–887.

Okada, Y., 1992. Internal deformation due to shear and tensile faults in a half space. Bulletin of the Seismological Society of America 82, 1018–1040.

Rice, J.R., Cleary, M.P., 1976. Some basic stress diffusion solutions for fluid-saturated elastic porous media with compressible constituents. Reviews of Geophysics 14, 227–241.

Robert, F., Poulsen, K.H., 2001. Vein formation and deformation in greenstone gold deposits. Society of Economic Geologists Reviews 14, 111–155.

Robert, F., Boullier, A.-M., Firdaous, K., 1995. Gold–quartz veins in metamorphic terranes and their bearing on the role of fluids in faulting. Journal of Geophysical Research 100, 12861–12881.

Roberts, D.E., Elias, M., 1990. Gold deposits of the St Ives–Kambalda region. In: Hughes, F.E. (Ed.), Geology and Mineral Deposits of Australia and Papua-New Guinea. The Australasian Institute of Mining and Metallurgy, Melbourne. pp. 479–491.

Roberts, R.G., 1987. Ore Deposit models #11, Archaean Lode Gold Deposits. Geoscience Canada 14, 37–51.

Sanderson, D.J., Zhang, X., 1999. Critical stress localization of flow associated with deformation of well fractured rock masses, with implications for mineral deposits. In: McCaffrey, K.J.W., Lonergan, L., Wilkinson, J.J. (Eds.) Fractures, Fluid Flow and Mineralisation. Geological Society of London, Special Publication 155, pp. 69–81.

Schwartz, D.P., Coppersmith, K.J., 1984. Fault behavior and characteristic earthquakes. Journal of Geophysical Research 89, 5681–5698.

Segall, P., Pollard, D.D., 1980. Mechanics of discontinuous faults. Journal of Geophysical Research 85, 4337–4350.

Sibson, R.H., 1985. A note on fault reactivation. Journal of Structural Geology 7, 751–754.

Sibson, R.H., 1986. Earthquakes and lineament infrastructure. Philosophical Transactions of the Royal Society, London A317, 63–79.

Sibson, R.H., 1990. Faulting and fluid flow. In: Nisbett, E. (Ed.), Short Course on Fluids in Tectonically Active Regimes in the Continental Crust. Mineralogical Association of Canada, Short Course Handbook 18, pp. 93–132.

Sibson, R.H., 2001. Seismogenic framework for hydrothermal transport and ore deposition. Society of Economic Geologists Reviews 14, 25–50.

Sibson, R.H., Robert, F., Poulsen, K.H., 1988. High-angle reverse faults, fluid pressure cycling, and mesothermal gold deposits. Geology 16, 551–555.

Stein, R.S., 1999. The role of stress transfer in earthquake occurrence. Nature 402, 605–609.

Stein, R.S., Barka, A.A., Dieterich, J.H., 1997. Progressive failure of the

North Anatolian fault since 1939 by earthquake stress triggering. Geophysical Journal International 128, 594–604.

Toda, S., Stein, R.S., Reasenberg, P.A., Dieterich, J.H., Yoshida, A., 1998. Stress transferred by the 1995 Mw = 6.9 Kobe, Japan, shock: effects of aftershocks and future earthquake probablilities. Journal of Geophysical Research 103, 24543–24565.

Wang, H.F., 1993. Quasi-static poroelastic parameters in rock and their geophysical applications. Pure and Applied Geophysics 141, 269–286.

Watchorn, R.B., 1998. Kambalda–St Ives gold deposits. In: Berkman, D.A., Mackenzie, D.H. (Eds.), Geology of Australian and Papua-New Guinea Ore Deposits, The Australasian Institute of Mining and Metallurgy, Melbourne, pp. 243–254.

Wells, D., Coppersmith, K., 1994. New empirical relationships among magnitude, rupture length, rupture width, rupture area and surface displacement. Bulletin of the Seismological Society of America 84, 974–1002.

Wesnousky, S.G., 1988. Seismological and structural evolution of strike-slip faults. Nature 335, 340–342.

Yeats, R.S., Sieh, K., Allen, C.R., 1997. The Geology of Earthquakes. Oxford University Press, New York.